

Enabling savings in silver consumption and poly-Si thickness by integration of plated Ni/Cu/Ag contacts for bifacial TOPCon solar cells

S. Kluska ^{a,*}, R. Haberstoh ^a, B. Grübel ^a, G. Cimotti ^a, C. Schmiga ^a, A.A. Brand ^a, A. Nägele ^a, B. Steinhäuser ^a, M. Kamp ^b, M. Passig ^b, M. Sieber ^b, D. Brunner ^b, S. Fox ^c

^a Fraunhofer Institute for Solar Energy Systems ISE, Germany

^b Rena Technologies GmbH, Germany

^c Jinko Solar Co. Ltd, Haining, China



A B S T R A C T

Plated Ni/Cu/Ag contacts offer the possibility to significantly reduce silver consumption for tunnel oxide passivated contact (TOPCon) solar cells. This work demonstrates industrial bifacial TOPCon solar cells with plated Ni/Cu/Ag metallization achieving champion solar cell efficiencies of up to 24.0%. The influence of reduced poly-Si thickness down to 60 nm of the TOPCon rear side on the open circuit voltage (V_{oc}) is analysed and the impact of laser-induced damage during laser contact opening (LCO) is characterized. Furthermore, mitigation strategies to systematic fill factor losses are developed including laser-induced nano-roughness within the LCO to increase contact adhesion and current-annealing to improve contact resistance.

1. Introduction

Resource availability becomes an increasingly important topic in the transition of a PV production market heading towards a multi terawatt production capacity in the next decade. Especially, silver for solar cell metallization turns out to be one of the critical materials in terms of availability and material costs [1,2]. The dependency on silver will even increase in an anticipated technology evolution from p-type passivated emitter and rear cells (PERC) to n-type solar cell concepts such as heterojunction or tunnel oxide passivated contact (TOPCon) solar cell in industry. State-of-the-art n-type solar cell designs with printed metal contacts typically require pastes on front and rear side with high silver content.

Laser structured and plated Ni/Cu contacts are an industrially feasible alternative to significantly reduce silver consumption for p- or n-type silicon solar cell designs. Recent works demonstrated successful integration of plated contacts for PERC [3], SHJ [4], PERT [5] and TOPCon. Grübel et al. [6,7] introduced a process sequence to realize bifacial TOPCon solar cells with plated Ni/Cu/Ag contacts. This sequence is applied in this work to metallize industrial TOPCon solar cells. This allowed to reduce the silver consumption to 4 mg per wafer or 0.6 mg/W compared to 130 mg for screen printed TOPCon solar cells in 2022 according to the International Technology Roadmap for Photovoltaic (ITRPV) [8].

The works of Arya [9] and Grübel [10] also indicate that the

application of plated contacts could enable to reduce the poly-Si thickness of the TOPCon rear side enabling further reductions in production cost by increased throughput of the poly-Si deposition.

This work demonstrates the application of laser structured and plated metal contacts on industrial type bifacial TOPCon solar cells with decreased poly-Si thickness on the TOPCon rear side down to approximately 60 nm. Furthermore, the aim of this work is to characterize the impact of the laser contact opening on the contact recombination of TOPCon rear side with reduced poly-Si thickness and develop strategies to ensure low contact resistances and reliable contact adhesion even on planarized surfaces.

2. Experimental

The TOPCon precursors used in this work were processed in an industrial R&D line and feature a variation in poly-Si thickness on the TOPCon rear side with thickness of 60 nm, 90 nm, 125 nm and 140 nm. The poly-Si thicknesses were confirmed with scanning electron microscope measurements at cross sections of the final solar cells after metallization. The fabrication process of the precursors is similar to the description of Grübel et al. [11]. The wafer area was 267.85 cm². The metallization process of the TOPCon solar cell precursors was either silver/silver-aluminum (Ag/AgAl) screen printing at the R&D line of the supplier or laser defined plated contacts fabricated at Fraunhofer ISE.

The plated solar cells feature an UV (355 nm laser wavelength)

* Corresponding author.

E-mail address: sven.kluska@ise.fraunhofer.de (S. Kluska).

picosecond (<15 ps) pulsed laser contact opening with an opening width of ~5 μm and 12 μm in diameter on the solar cell front and rear side, respectively. The LCO pulse pitch within the finger line was set to 90% of the LCO diameter. The finger lines featured a finger pitch of 1 mm and 9 busbar were applied with a busbar width of 50 μm in average. After LCO formation the laser damage was cured in an industrial type fast firing process (FFO) using a fast firing system by Rehm Thermal Systems with belt speed of 6 m/min and a set peak temperature of 870 °C. Laser-induced and native oxide layer within the LCO were removed with a single side 1.5% HF pre-treatment (30 s) prior to the single side inline plating process. Lab type single lane inline plating tools similar to the In Cell Plate platform supplied by Rena Technologies GmbH were used to plate a stack of Ni (~0.5 μm)/Cu(5–10 μm)/Ag(<0.5 μm). The nickel (Nimate PV) and copper (Cupracid PV 5–2) electrolyte used in this experiment were supplied by Atotech Group. Plating on the n-type TOPCon and p-type emitter side was performed with light-induced plating (current controlled) and forward bias plating (current controlled), respectively. The set current density for nickel deposition was 2.5 A/dm² (front side) and 2.2 A/dm² (rear side) and for copper 15.2 A/dm² (front side) and 11.5 A/dm² (rear side). The silver capping layer was chemically deposited in an immersion plating process.

The experiment design is illustrated in Fig. 1. Solar cells with either plated or screen printed metallization were fabricated for each poly-Si thickness. Furthermore, LCO test samples were processed using LCO line patterns with increasing laser pulse energy similar to Arya et al. [9]. Each processing group featured at least 10 solar cells per metallization.

The fabricated solar cells were characterized using an industrial type IV flasher with a non reflective chuck and a grid neglecting contacting unit (see appendix A of [12]). After IV testing laser-enhanced contact optimization (LECO) [13] was applied to the solar cells. During the process a laser scans the over the cells front side which causes a very high local injection of charge carriers. At the same time a negative bias voltage is applied to the contacts of the cell. The high injection and the negative bias voltage cause high current densities through the contact interface, which are responsible for contact formation and hence improve the metal semiconductor contact of the cells.

The champion solar cells were externally characterized at Fraunhofer ISE Callab using calibrated IV measurements with a

reflective chuck and a grid neglecting contacting unit. Please note that the champion solar cells featured exactly the same processing sequence as all other solar cells and were selected after IV flash testing without any modification before the calibrated measurement. Furthermore, all solar cells were characterized using electroluminescence (EL) and photoluminescence (PL) imaging. EL imaging at a current of 10 A was used in this work to indicate regions with hindered electrical current distribution. Locally increased series resistances are among other reasons one of the most common origins of decreased EL intensity in these areas. Photoluminescence measurements were performed at 1 sun illumination. Locally decreased PL intensities are used in this work to locate regions of increased recombination activity.

3. Results & discussion

3.1. Analysis of champion solar cells

The IV results of the champion solar cells with each metallization approach are summarized in Table 1. The narrow front side contact width (~15 μm contact width, 5 μm LCO width) of the plated TOPCon solar cells allowed low contact shading (+0.3 mA/cm² compared to SP reference) and low front side contact recombination (+10 mV compared to SP reference). The low contact resistivity of plated nickel on boron doped emitters and phosphorous doped TOPCon allowed low series resistance-induced losses of the fill factor (FF) even for the narrow front side laser contact opening width of 5 μm .

Table 1

Calibrated IV measurements of champion TOPCon solar cells (poly thickness: 125 nm) with plated and screen printed metallization measured at Fraunhofer ISE Callab.

Metallization	η (%)	J_{sc} (mA/cm ²)	V_{oc} (mV)	FF (%)
Ag/AgAl screen printing	23.5	40.7	705	81.9
Plated Ni/Cu/Ag	24.0	41.0	715	82.0

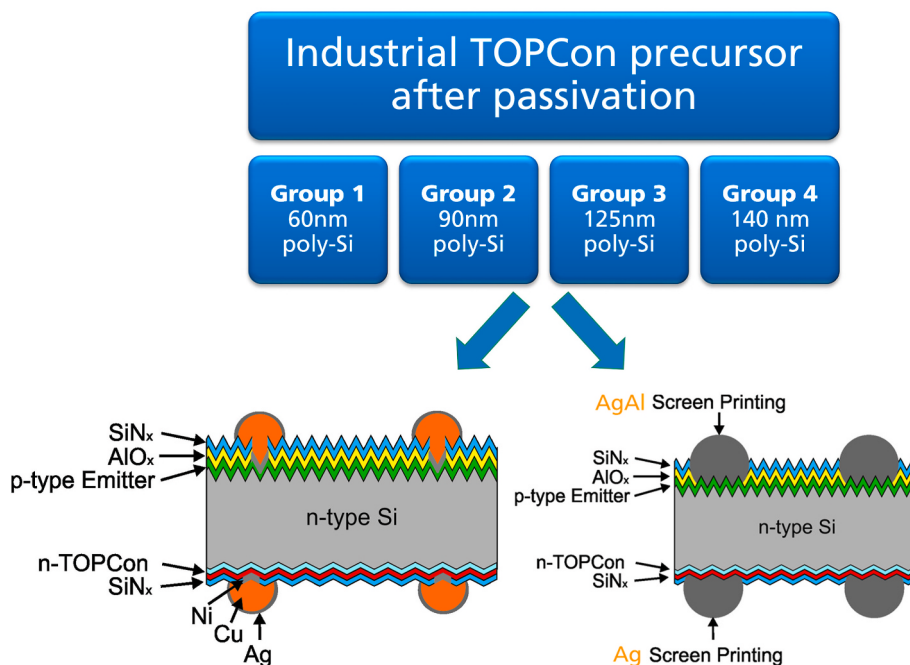


Fig. 1. Cross sections of the fabricated TOPCon solar cells based on industrial TOPCon precursors with variations in poly-Si thickness on the rear side. Please note that all solar cells featured on front and rear side either plated or screen printed contacts.

3.2. V_{oc} characteristics and contact recombination

Fig. 2 shows the V_{oc} distribution of the solar cells for each metallization approach related to the poly-Si thickness variation for the TOPCon rear side. The V_{oc} advantage of the plated solar cells compared to the screen printed ones is in a range of 5–10 mV. Grübel et al. [11] demonstrated that the main limitation in V_{oc} of plated TOPCon solar cells (similar to the one used in this experiment) is caused by contact recombination of the front side emitter contact. Grübel estimates the saturation current density of a laser ablated and plated emitter contact to be in the range of 1000–3000 fA/cm². The following section shows that the contact recombination contribution of the TOPCon contact is in this work for laser ablation close to the ablation threshold usually below these values even for reduced poly-Si thickness of 60 nm.

Calibrated Photoluminescence imaging of the implied V_{oc} with and w/o laser contact openings are used to evaluate the LCO induced rear side contact recombination. Fig. 3 shows the LCO-induced iV_{oc} loss (after LCO and FFO annealing) for test structures with three different poly-Si thicknesses and increasing laser pulse energy. Please note that all LCO pulse energies in Fig. 3 provide a full area LCO with an opening width of 12–18 μ m, which are all applicable for solar cell fabrication.

The marked data refers to a similar LCO used for solar cell fabrication. No significant iV_{oc} reduction was measured for the 125 nm poly Si thickness even for large LCO pulse energies. The threshold in laser pulse energy which leads to LCO-induced iV_{oc} losses is seen for poly Si thickness of 90 nm and below. However, the applicable range of LCO pulse energies with no significant iV_{oc} degradation is for all poly-Si thicknesses still well above the ablation threshold. The applied LCO pulse energy of the solar cells in Fig. 3 is for all poly-Si thickness in a region of no significant iV_{oc} reduction. The LCO design of the PL test structures featured a contact fraction of ~1%. The iV_{oc} degradation in Fig. 3 in the range of ~1–8 mV correlates to a saturation current density of the rear side contact $J_{0,LCO}$ of 200–1500 fA/cm², respectively. This range in $J_{0,LCO}$ equals the findings of Arya et al. [9] on similar poly-Si thicknesses. However, the data of this work suggests that even for 60 nm poly-Si thickness low iV_{oc} degradation (≤ 1 mV (referring to $J_{0,LCO} \leq 200$ fA/cm²) are possible. This suggests that even thinner poly-Si thicknesses would be applicable for TOPCon solar cells with a laser structured and plated metallization approach without significant V_{oc}

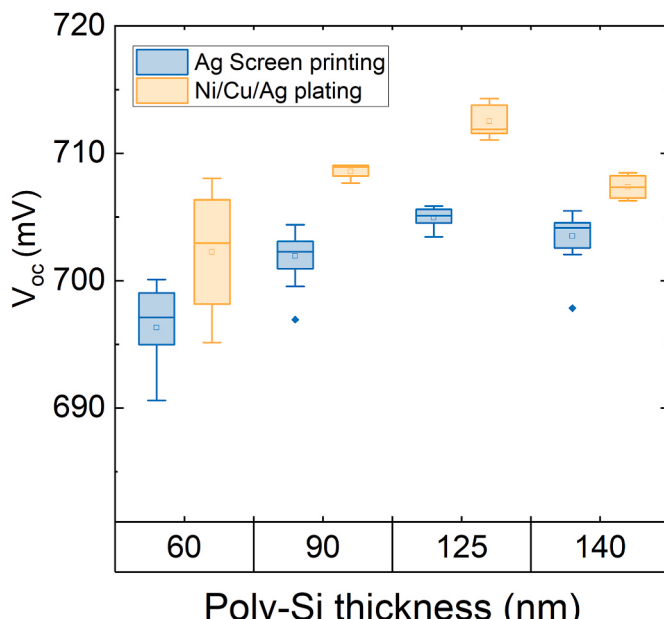


Fig. 2. V_{oc} measurements of plated and screen printed TOPCon solar cells with a variation in poly-Si thickness of the TOPCon rear side.

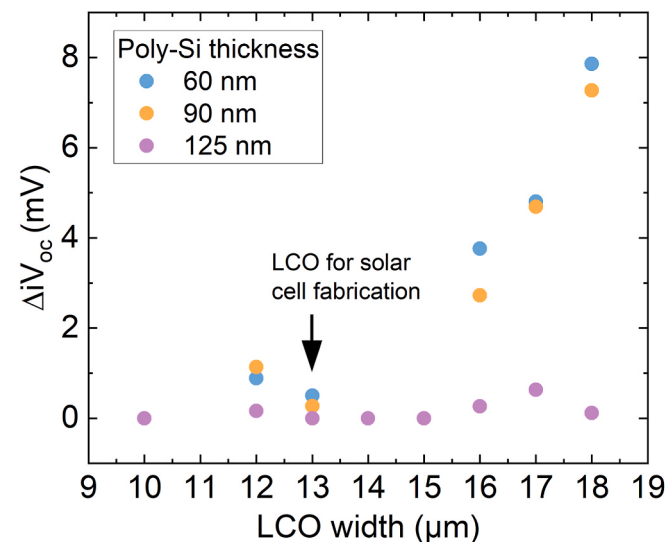


Fig. 3. Measured iV_{oc} loss of the rear side (TOPCon) LCO formation (after FFO annealing).

losses.

3.3. Series resistance and fill factor characteristics

The IV measurements of the whole data set of plated solar cells revealed in this experiment large FF spreading in the range of 50–83%. Optical inspection and EL measurements allowed to categorize solar cells with decreased FF compared to the screen printed references. Two reasons for this could be identified for the plated groups. First, solar cells with locally low contact adhesion on the rear side, leading to significant drops in FF well below 80% and large areas with low EL intensity. Second, minor deviations in FF in the range of 77–82% compared to the plated champion solar cell and local spots with low EL intensity. These kinds of defects were sensitive on LECO current annealing, which lead to an increase in FF by 1–2%abs.

In the following the microscopic origins and mitigation strategies for both error types are discussed.

3.3.1. Nano-roughness as adhesion promoter of plated contacts on etched back surfaces

Scanning electron microscopy was used to characterize differences of the LCO for solar cells with and without contact adhesion failures. Fig. 4 shows false color SEM images (in Viridis color scale [14]) of representative LCO for each case.

The silicon surface of solar cells with contact adhesion failures shows no significant exploits laser-induced periodic surface structures (LIPSS) within the LCO Fig. 4 a). The LCO of solar cells with no contact adhesion failures and FF above 80% shows LIPSS Fig. 4 b). The origin of these differences in LCO formation are still under investigation. Further characterizations demonstrated that LIPSS can also be manufactured on samples with a planarized surface after alkaline chemical edge isolation Fig. 4 c).

Different approaches are known from literature to achieve a reliable contact adhesion for plated contacts on silicon. The most famous approaches are plating on metallic seed layers (e.g. PVD metal layers such as TiPdAg, Ti, Mo), galvanic surface displacement (electrochemically deposited seeds such as Pd [15] or Ni [5] silicidation of the nickel-silicon interface [16], and/or laser-induced nano-roughness [17]. The last one exploits LIPSS, which result from interference of ultra-short laser pulses on the pyramid texture of a solar cell.

The classification and analysis of the solar cells with missing contact adhesion in this experiment was performed before current annealing.

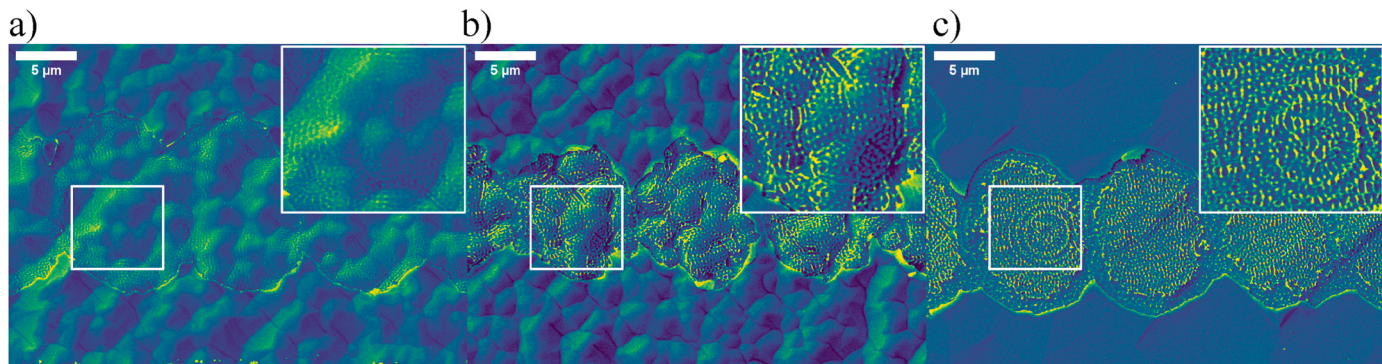


Fig. 4. False color SEM images of laser contact openings with and w/o LIPSS on TOPCon surfaces with acidic emitter etch back (a/b) and alkaline etch back (c).

Therefore, the only mechanism to achieve contact adhesion was the laser-induced nano-roughness visible in Fig. 4 (b,c). Further investigations are ongoing how sample properties such as surface morphology, passivation layer and LCO parameters are influencing the appearance of LIPSS on chemically polished TOPCon surfaces.

The current results demonstrate that the approach of laser-induced roughness for increased contact adhesion is applicable even on planarized surfaces but that a proper process control is necessary to avoid contact adhesion failures. Furthermore, it is expected that the combination of LIPSS and another approach such as annealing-induced silicidation are beneficial to improve contact adhesion reliability on planarized surfaces in an industrial environment.

3.3.2. Current annealing induced contact resistance improvement of plated contacts

The second type of decreased FF is summarized in the orange data in Fig. 5 and shows a range of 78–81%: The application of a current annealing process (LECO) lead to a mean improvement in FF of about 1.5%_{abs}. Series resistance (R_s) characterization showed that the R_s could be reduced by about 0.3 Ωcm² after LECO with lower variation in R_s . No significant changes in grid resistance were measured before and after LECO.

The detailed analysis of the V_{oc} , and series resistance (R_s) change of each cell after LECO is presented in Fig. 6. A decrease in R_s correlates to a slight decrease in V_{oc} . The same is true for decreased R_s correlating to slight decrease in pFF in the range of up to 0.15%_{abs} (not shown here). These results indicate that the origin of the series resistance/FF improvements also lead to an increased recombination activity (decreased V_{oc} /pFF). Further local imaging techniques are used to analyse local changes in electroluminescence (EL) and photoluminescence (PL)

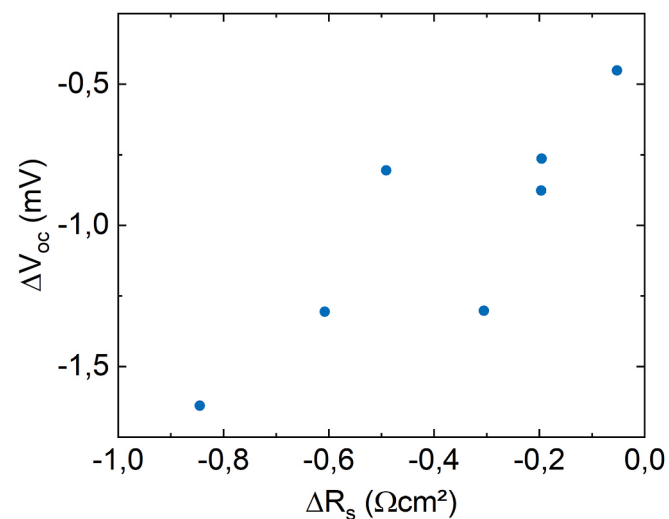


Fig. 6. Measured changes in V_{oc} , and R_s for each solar cell after LECO.

before/after LECO.

Fig. 7 shows EL and PL measurements before and after LECO for 3 representative solar cells with plated contacts. A selection of local features are marked to compare the changes before/after LECO annealing.

Feature F1 shows a larger cloudy area with low EL intensity before LECO with 2 vertical lines with increased EL intensity, which correlate to busbar positions on the rear side. After LECO the contacting improves resulting in an increased and more homogeneous EL signal in F1. The

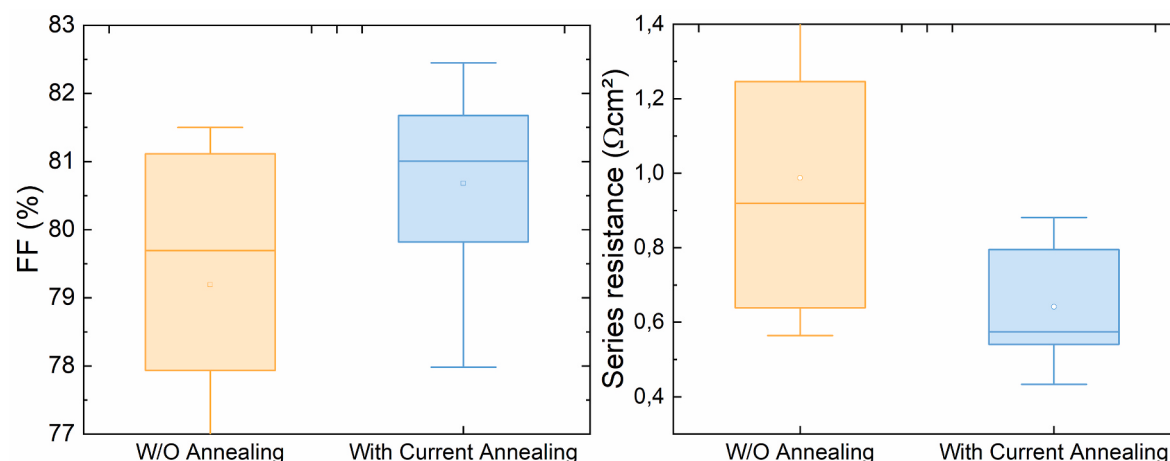


Fig. 5. Mean changes in FF and series resistance before and after current annealing (LECO).

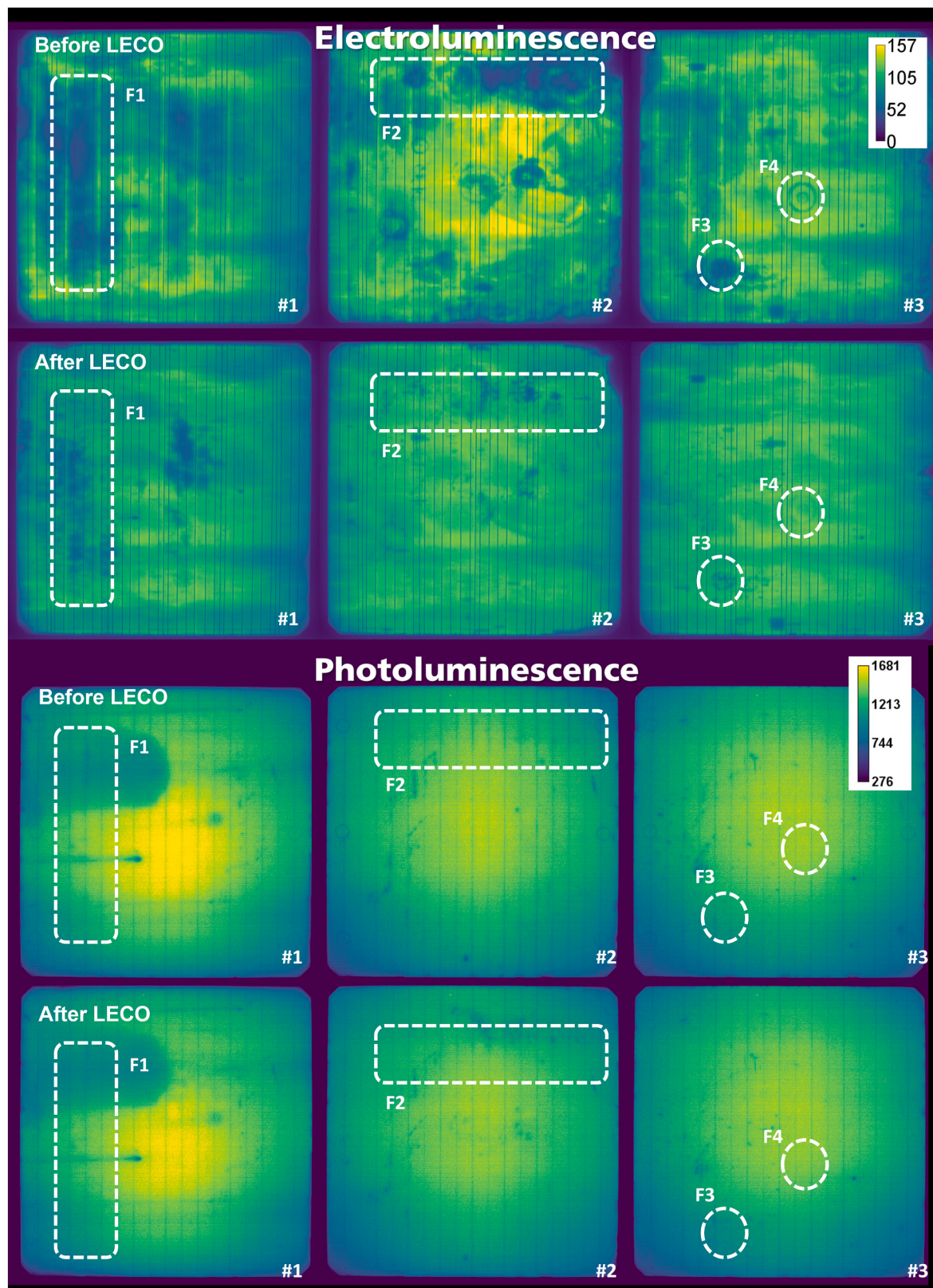


Fig. 7. EL and PL measurements of three representative TOPCon solar cells with plated contacts before and after LECO.

photoluminescence image shows no significant change before/after LECO.

Feature F2 shows local regions with decreased EL intensity with shapes related to automation handling marks and larger cloudy areas in the surrounding. Most of the features in F2 disappear after LECO. Only

local spots with decreased intensity remain in F2 after LECO. These local spots are not visible in PL before LECO but appear in PL after LECO.

Feature F3 and F4 in EL are also correlated to automation handling marks. Again, the EL intensity in these areas is increased and homogenized after LECO. In contrast to F2 the PL shows no change before/after

LECO.

EL characterization shows mainly improvements in local features after LECO. The origin of this annealing-induced FF improvement is expected to be caused by changes in the contact resistance of the nickel-silicon interface in these areas. At the same time PL imaging reveals that at some (but not all) positions the improvements in EL signal correlate with local decrease in PL (new local recombination features) after LECO.

LECO is known to change the contact interface by creating metal-silicon spikes due to locally increased temperatures during the current annealing [18]. These local temperature increase can act twofold at the Ni-Si interface. Temperatures above 200 °C would enable nickel silicide growth assuming an oxide free Ni-Si interface. The locally formed silicide spike would improve contact resistance (increased EL signal, FF increase) and -depending on its depth-locally increase contact recombination (decreased PL, decreased V_{oc}). Especially on the emitter side this would also result in local non-ohmic shunts (pFF decrease) [19]. Furthermore, the high local current densities in the range of MA/cm^2 [18] are likely to cause an electrical breakdown of remaining interface oxide, oxi-nitride or nitride layers [20] at the Ni-Si interface [21] resulting in increased contact area (decreased contact resistance, increased contact recombination).

4. Conclusion

This work demonstrated that the application of a plated Ni/Cu/Ag metallization approach is able to significantly reduce silver consumption for industrial TOPCon solar cells and at the same time achieve high cell efficiencies of up to 24%. Furthermore, the application of UV-ps LCO allows to achieve low contact recombination on the TOPCon rear side. This held to be true even for reduced poly-Si thickness down to 60 nm. A maximum V_{oc} of up to 708 mV was achieved on 60 nm poly-Si using a plated metallization approach. A detailed study of the rear side contact recombination revealed the potential to further reduce the poly-Si thickness on the TOPCon rear side for the case of plated metal contacts. Microscopic analysis allowed to identify laser-induced nano structures within the LCO as crucial element to achieve contact adhesion of plated contacts on planarized surfaces. Furthermore, it could be shown that the application of current-induced annealing by the LECO process improves the contact resistance of plated contacts in TOPCon solar cells.

Further investigations are necessary to characterize the rear side contact recombination of plated contacts in TOPCon solar cells for poly-Si thicknesses below 60 nm. Moreover, further investigations are required to identify the influencing factors to achieve laser-induced periodic surface structures within the laser contact openings on planarized surfaces.

CRediT authorship contribution statement

S. Kluska: Writing – original draft, Supervision, Project administration, Methodology, Investigation, Funding acquisition, Formal analysis, Conceptualization. **R. Haberstoh:** Writing – review & editing, Investigation, Data curation. **B. Grübel:** Writing – review & editing, Formal analysis, Data curation, Conceptualization. **G. Cimotti:** Investigation. **C. Schmiga:** Writing – review & editing, Investigation, Formal analysis, Data curation, Conceptualization. **A.A. Brand:** Writing – review & editing, Investigation. **A. Nägele:** Investigation. **B. Steinhauser:** Writing – review & editing, Investigation, Data curation, Conceptualization. **M. Kamp:** Writing – review & editing, Resources, Investigation, Conceptualization. **M. Passig:** Writing – review & editing, Resources. **M. Sieber:** Writing – review & editing, Resources, Conceptualization. **D. Brunner:** Writing – review & editing, Resources, Investigation, Funding acquisition, Conceptualization. **S. Fox:** Writing – review & editing, Resources, Conceptualization.

Declaration of competing interest

The authors declare that they have no known competing financial interests or personal relationships that could have appeared to influence the work reported in this paper.

Data availability

The authors are unable or have chosen not to specify which data has been used.

Acknowledgements

This work was funded by the German Federal Ministry for Economic Affairs and Climate Action within the research projects “TALER” (contract no. 03EE1021B) and “TOPConCluster” (contract no. 03EE1065A). The authors want to thank the colleagues at Fraunhofer ISE for their support in preparation and processing of the solar cells.

References

- [1] Y. Zhang, M. Kim, L. Wang, P. Verlinden, B. Hallam, Design Considerations for Multi-Terawatt Scale Manufacturing of Existing and Future Photovoltaic Technologies: Challenges and Opportunities Related to Silver, Indium and Bismuth Consumption, Energy & Environmental Science, 2021, <https://doi.org/10.1039/D1EE01814K>.
- [2] P.J. Verlinden, Future challenges for photovoltaic manufacturing at the terawatt level, J. Renew. Sustain. Energy 12 (2020), 53505, <https://doi.org/10.1063/5.0020380>.
- [3] J.T. Horzel, Y. Shengzhao, N. Bay, M. Passig, D. Pysch, H. Kuhnlein, H. Nussbaumer, P. Verlinden, Industrial Si solar cells with Cu-based plated contacts, IEEE J. Photovolt. 5 (2015) 1595–1600, <https://doi.org/10.1109/JPHOTOV.2015.2478067>.
- [4] A. Lachowicz, Review on Plating Processes for Silicon Heterojunction Cells, Konstanz, 2018. http://www.metallizationworkshop.info/fileadmin/metallizationworkshop/presentations2019/5.2_Lachowicz_20190530_MIW_ReviewCuPlatingHJTCells.pdf. (Accessed 3 January 2020).
- [5] L. Tous, R. Russell, E. Cornagliotti, A. Uruena, P. Choulat, M. Haslinger, J. John, F. Duerinckx, J. Szlufcik, 22.4% bifacial n-PERT cells with Ni/Ag co-plated contacts and V_{oc} of ~691 mV, Energy Proc. 124 (2017) 922–929, <https://doi.org/10.1016/j.egypro.2017.09.292>.
- [6] B. Grübel, G. Cimotti, V. Arya, T. Fellmeth, F. Feldmann, B. Steinhauser, S. Kluska, T. Kluge, D. Landgraf, M. Glatthaar, Plated Ni/Cu/Ag for TOPCon solar cell metallization, in: Proceedings of the 36th European Photovoltaic Solar Energy Conference and Exhibition, EU PVSEC.
- [7] B. Grübel, G. Cimotti, C. Schmiga, V. Arya, B. Steinhauser, N. Bay, M. Passig, D. Brunner, M. Glatthaar, S. Kluska, Direct contact electroplating sequence without initial seed layer for bifacial TOPCon solar cell metallization, IEEE J. Photovolt. 11 (2021) 584–590, <https://doi.org/10.1109/jphotov.2021.3051636>.
- [8] ITRPV Consortium, International Technology Roadmap for Photovoltaic (ITRPV): Results 2020, twelfth ed. twelfth ed., tenth ed., 2021.
- [9] V. Arya, B. Steinhauser, B. Grübel, C. Schmiga, N. Bay, D. Brunner, M. Passig, A. A. Brand, S. Kluska, J. Nekarda, Laser ablation and Ni/Cu plating approach for TOPCon solar cells with variate polysilicon layer thickness: gains and possibilities in comparison to screen printing, Phys. Status Solid. A 217 (2000474) (2020) 1–9, <https://doi.org/10.1002/pssa.202000474>.
- [10] B. Grübel, H. Nagel, B. Steinhauser, F. Feldmann, S. Kluska, M. Hermle, Influence of plasma-enhanced chemical vapor deposition poly-Si layer thickness on the wrap-around and the quantum efficiency of bifacial n-TOPCon (tunnel oxide passivated contact) solar cells, Phys. Status Solid. A 218 (2021), 2100156, <https://doi.org/10.1002/pssa.202100156>.
- [11] B. Grübel, G. Cimotti, C. Schmiga, S. Schellinger, B. Steinhauser, A.A. Brand, M. Kamp, M. Sieber, D. Brunner, S. Fox, S. Kluska, Progress of plated metallization for industrial bifacial TOPCon silicon solar cells, Prog Photovoltaics 3528 (2021), <https://doi.org/10.1002/pip.3528>.
- [12] M.A. Green, E.D. Dunlop, J. Hohl-Ebinger, M. Yoshita, N. Kopidakis, K. Bothe, D. Hinken, M. Rauer, X. Hao, Solar cell efficiency tables (Version 60), Prog Photovoltaics 30 (2022) 687–701, <https://doi.org/10.1002/pip.3595>.
- [13] E. Krassowski, S. Großer, M. Turek, A. Henning, H. Zhao, Investigation of monocrystalline p-type PERC cells featuring the laser enhanced contact optimization process and new LECO paste, in: AIP Conference Proceedings, vol. 2367, 2021, 20005, <https://doi.org/10.1063/5.0056380>.
- [14] Simon Garnier, Noam Ross, boB. Rudis, Antoine Filipovic-Pierucci, Tal Galili, timelyportfolio, Brandon Greenwell, Carson Sievert, David J. Harris, J.J. Chen, Sjmgarnier/Viridis: Viridis 0.6.0 (Pre-CRAN Release), 2021. Zenodo.
- [15] R.A. Pryor, Metallization of Large Silicon Wafers, 1979. Final report.
- [16] A. Mondon, M.N. Jawaid, J. Bartsch, M. Glatthaar, S.W. Glunz, Microstructure analysis of the interface situation and adhesion of thermally formed nickel silicide for plated nickel-copper contacts on silicon solar cells, Sol. Energy Mater. Sol. Cell. 117 (2013) 209–213, <https://doi.org/10.1016/j.solmat.2013.06.005>.

- [17] A. Büchler, Interface Study on Laser-Structured Plated Contacts for Silicon Solar Cells, Dissertation, Stuttgart, 2019.
- [18] S. Groser, E. Krassowski, S. Swatek, H. Zhao, C. Hagendorf, Microscale contact formation by laser enhanced contact optimization, *IEEE J. Photovolt.* 12 (2022) 26–30, <https://doi.org/10.1109/jphotov.2021.3129362>.
- [19] A. Büchler, S. Kluska, M. Kasemann, M. Breitwieser, W. Kwapił, A. Hähnel, H. Blumtritt, S. Hopman, M. Glatthaar, Localization and characterization of annealing-induced shunts in Ni-plated monocrystalline silicon solar cells, *Phys. Status Solidi RRL* 8 (2014) 385–389, <https://doi.org/10.1002/pssr.201409036>.
- [20] X. Shen, P.C. Hsiao, B. Phua, A. Stokes, V.R. Gonçales, A. Lennon, Plated metal adhesion to picosecond laser-ablated silicon solar cells: influence of surface chemistry and wettability, *Sol. Energy Mater. Sol. Cell.* 205 (110285) (2020), <https://doi.org/10.1016/j.solmat.2019.110285>.
- [21] S. Kluska, A. Büchler, J. Bartsch, B. Grubel, A.A. Brand, S. Gutscher, G. Cimotti, J. Nekarda, M. Glatthaar, Easy plating—a simple approach to suppress parasitically metallized areas in front side Ni/Cu plated crystalline Si solar cells, *IEEE J. Photovoltaics* 7 (2017) 1270–1277, <https://doi.org/10.1109/JPHOTOV.2017.2720461>.